Australian Meteorological and Oceanographic Journal 62 (2012) 39–50

Seasonal climate summary southern hemisphere (autumn 2011): one of the strongest La Niña events on record begins to decline

S. Tobin[1] and T.C.L. Skinner[2]
[1]National Climate Centre, Bureau of Meteorology, Australia
[2]National Meteorological & Oceanographic Centre, Bureau of Meteorology, Australia

(Manuscript received May 2012)

Southern hemisphere circulation patterns and associated anomalies for the austral autumn 2011 are reviewed, with emphasis given to the Pacific Basin climate indicators and Australian rainfall and temperature patterns. Early autumn saw the continuation of the strong La Niña conditions that had been evident during the latter half of 2010. ENSO indices during March and April showed a strong La Niña signature prior to a rapid decline to neutral conditions in May. The April Southern Oscillation Index value was the second-highest for any month since November 1973. Averaged nationally over the Australian continent and Tasmania, rainfall for autumn was the fourth-highest on record and highest since 2000, with falls over the Northern Territory exceeding the previous highest area-averaged total. In contrast, there were continuing rainfall deficiencies over the western half of Western Australia. Australia-wide mean temperatures were lowest on record, as were mean temperatures for the Northern Territory, and for Queensland as a whole.

Introduction

This summary reviews the southern hemisphere and equatorial climate patterns for autumn 2011, with particular attention given to the Australasian and Pacific regions. The main sources of information for this report are analyses prepared by the Bureau of Meteorology's National Climate Centre and the Centre for Australian Weather and Climate Research (CAWCR).

Pacific Basin climate indices

Southern Oscillation Index (SOI)

Strong positive values of the Troup Southern Oscillation Index[1] (SOI) which began in winter 2010 continued throughout summer 2010–11 and persisted well into autumn 2011. Monthly values were +21.4 (March), +25.1 (April), and +2.1 (May). The April SOI value was the second-highest on record for any month since November 1973 (+31.6), and the second-highest for any April on record (the highest April value was +31.7 in 1904). The average September to April SOI (+21.9) was the highest on record for this period, exceeding the La Niña of 1917–18 (+16.8) and the La Niña of 1973–74 (+17.5) The high SOI values are representative of the strong La Niña event in the Pacific which developed in autumn 2010 (Ganter 2011) and continued until autumn 2011 (Lovitt 2011, Imielska 2011). Figure 1 shows the monthly SOI from January 2008 to May 2011, together with a five-month weighted moving average.

Composite monthly ENSO index (5VAR)

5VAR[2] is a composite monthly ENSO index, calculated as the standardised amplitude of the first principal component of monthly Darwin and Tahiti mean sea level pressure (MSLP)[3] and monthly NINO3, NINO3.4 and NINO4 sea surface

[1]The Troup Southern Oscillation Index (Troup 1965) used in this article is ten times the standardised monthly anomaly of the difference in mean sea level pressure (MSLP) between Tahiti and Darwin. The calculation is based on a sixty-year climatology (1933–1992). The Darwin MSLP is provided by the Bureau of Meteorology, with the Tahiti MSLP being provided by Météo France inter-regional direction for French Polynesia.

Corresponding author address: S.Tobin, National Climate Centre, Bureau of Meteorology, PO Box 1289, Melbourne Vic. 3001, Australia
email: s.tobin@bom.gov.au

[2]ENSO 5VAR was developed at the Bureau's National Climate Centre and is described in Kuleshov et al. (2009). The principal component analysis and standardisation of this ENSO index is performed over the period 1950–1999.

[3]MSLP data obtained from http://www.bom.gov.au/climate/current/soihtm1.shtml. As previously mentioned, the Tahiti MSLP data are provided by Météo France inter-regional direction for French Polynesia.

Fig. 1 Southern Oscillation Index, from January 2008 to May 2011, together with a five-month binomially weighted moving average. Means and standard deviations used in the computation of the SOI are based on the period 1933–1992.

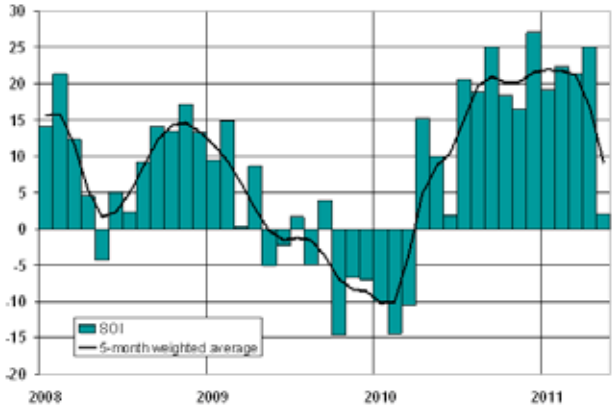

Fig. 2 5VAR composite standardised monthly ENSO index from January 2008 to May 2011, together with a weighted three-month moving average. See text for details.

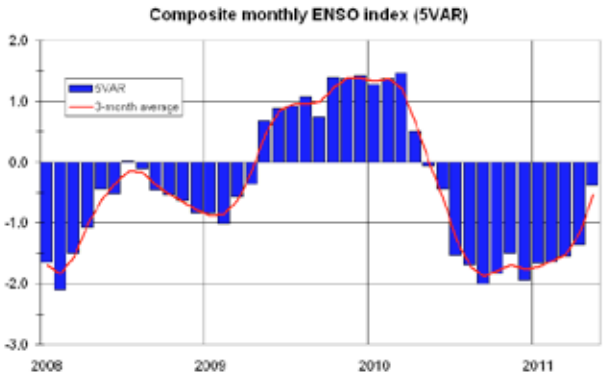

temperatures[4] (SSTs).The sequence of negative 5VAR values which began in winter 2010 continued during autumn 2011 (Fig. 2).

Figure 2 shows a steep rise in the 5VAR value for May, moving towards neutral values following strong negative values in the preceding months. 5VAR had been strongly negative since the latter half of 2010. The monthly values for this index were –1.55 (March), –1.36 (April), and –0.38 (May). Values of 5VAR between spring 2010 and early autumn 2011 exceeded one standard deviation.

The Multivariate ENSO Index[5] (MEI), produced by the US Climate Diagnostics Center, is derived from a number of atmospheric and oceanic parameters, which are typically associated with ENSO, and is calculated as a two-month mean. Significant negative values indicate La Niña, while significant positive values indicate El Niño. The MEI values have been ranked over the 62-year record, beginning in 1950. The lowest value (1) signifies the strongest La Niña case for that particular two-month pairing, while the highest number (62) signifies the strongest El Niño case. By the end of winter 2010, the MEI reached –2.04 (bimonthly August–September 2010 value), the lowest value on record for that time of year and tied with July–August 1955 for the lowest value on record (since 1950). The autumn 2011 values were –1.56 (February–March), –1.50 (March–April), and –0.37 (April–May) signifying a weakening of the formerly strong La Niña conditions. The first two periods both ranked fourth-lowest for their respective bimonthly historical MEI values.

Outgoing long-wave radiation

Outgoing long-wave radiation (OLR) over the equatorial Pacific near the Date Line (5ºS to 5ºN and 160ºE to 160ºW) is a good measure of tropical deep convection; increases (decreases) in OLR indicate decreases (increases) in convection and associated cloudiness. During La Niña events, OLR near the Date Line is often above average, indicating that convection is suppressed over this region. El Niño events, on the other hand, usually exhibit below-average OLR near the Date Line, meaning convection is generally enhanced over this region. The Climate Prediction Center, Washington, computes a standardised monthly anomaly[6] of OLR over this region of the equatorial Pacific. Monthly values for March, April and May were +1.7, +1.1, and +0.2 respectively. The decreasing positive values are consistent with weakening La Niña conditions, and indicate that convection over the equatorial Pacific near the Date Line was increasing (returning from suppressed to near-normal levels) during the latter half of autumn.

The spatial pattern of seasonal OLR anomalies across the Asia–Pacific tropics for autumn 2011 is shown in Fig. 3. Consistent with the standardised anomalies discussed above, strong positive anomalies were present in the equatorial Pacific, just west of the Date Line, while very strong negative OLR anomalies were present over Indonesia and the northwest Pacific. The strong negative anomalies over the northwest Pacific are a reflection of the active monsoon trough which developed in the area during April. Typhoon *Songda* developed during mid- to late May into an intense cyclone to the east of the Philippines. Negative OLR anomalies were evident over northern Australia. This reflected the well-above-normal rainfalls over large areas of the continent during March, which contrasted with the well-below-normal rainfall recorded over the southwest of Western Australia.

Madden-Julian Oscillation

The Madden-Julian Oscillation (MJO) is a tropical

[4]SST indices obtained from ftp://ftp.cpc.ncep.noaa.gov/wd52dg/data/indices/sstoi.indices.

[5]Multivariate ENSO Index obtained from http://www.esrl.noaa.gov/psd/people/klaus.wolter/MEI/table.html. The MEI is a standardised anomaly index described in Wolter and Timlin 1993, and 1998.

[6]Standardised monthly OLR anomaly data obtained from http://www.cpc.ncep.noaa.gov/data/indices/olr

Fig. 3 OLR anomalies for autumn 2011 (W m^{-2}). Base period 1979–1998. The mapped region extends from 40°S to 40°N and from 70°E to 180°E.

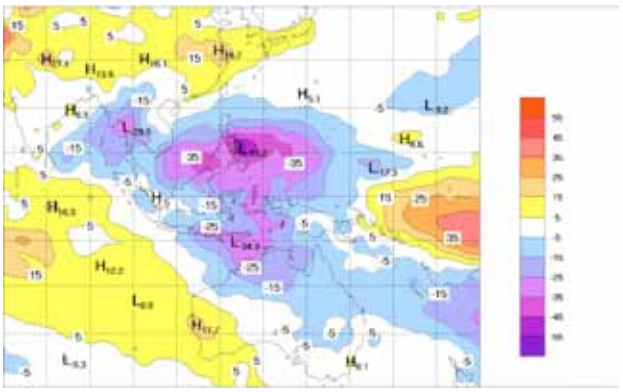

Fig. 4 Time-longitude section of seven-day running mean OLR anomalies, averaged for 15°S to 15°N, for the period December 2010 through to June 2011. Anomalies are with respect to a base period of 1979–2001.

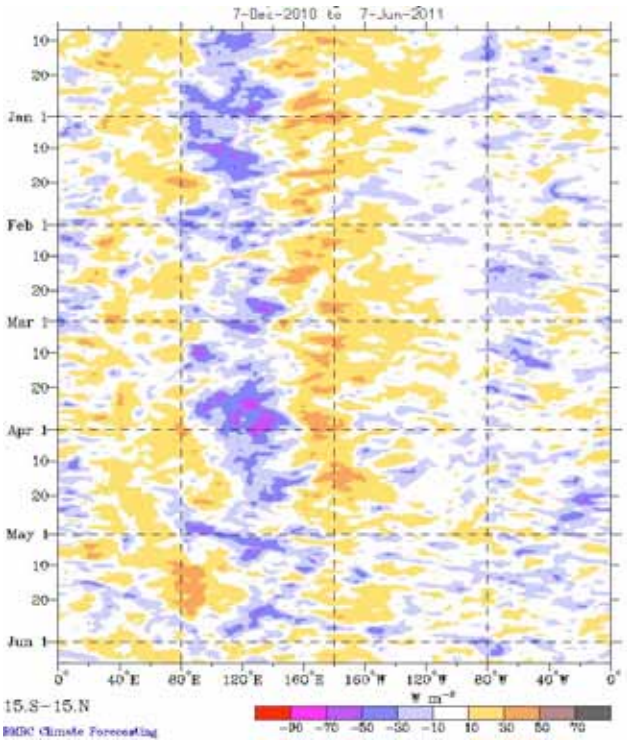

atmospheric anomaly which develops in the Indian Ocean and propagates eastwards into the Pacific Ocean (Zhang 2005). The MJO takes approximately 30 to 60 days to reach the western Pacific, with a frequency of six to twelve events per year (Donald et al. 2004). When the MJO is in an active phase, it is associated with increased tropical rainfall, with the effects mainly concentrated during early autumn. The evolution of tropical convection anomalies along the equator with time is shown in Fig. 4, starting from December 2010, through to June 2011. In the daily-averaged OLR anomalies shown in Fig. 4, the MJO became active in the Indian Ocean in mid-March and progressed into the Maritime Continent towards the end of March as a very active system, prior to moving into the west Pacific and weakening in early April. The next active phase of the MJO became evident during late April over the Indian Ocean before progressing across the Maritime Continent into the western Pacific during May. For a discussion of the impacts of the MJO on Australian rainfall see Wheeler et al. (2009).

As discussed in the previous section, positive OLR anomalies with fluctuating amplitudes over the central equatorial Pacific may also be seen in Fig. 4. These positive anomalies are associated with La Niña conditions, and became established during autumn and winter 2010.

Oceanic patterns

Sea surface temperatures

Autumn 2011 global sea surface temperature (SST) anomalies, from the US National and Oceanic and Atmospheric Administration Optimum Interpolation analysis (Reynolds et al. 2002), are displayed in Fig. 5, in degrees Celsius (°C). Positive (warm) anomalies are shown in red shades, while negative (cool) anomalies are shown in blue shades. Summer 2010–11 SSTs remained at strong La Niña levels and peaked during January (Imielska 2011). The cool anomalies in the central and eastern tropical Pacific Ocean that had been evident since the middle of 2010 warmed slightly, signalling the decay of the La Niña during autumn which is consistent with the historical demise of previous El Niño/La Niña events. In March warm anomalies appeared in the far eastern equatorial Pacific (Fig. 5) and persisted till the end of autumn. Anomalies of –1.0 °C to –1.5 °C prevailed on either side of the Equator with negative anomalies extending to higher latitudes in the eastern Pacific. SSTs surrounding Australian tropical coasts started to cool in March and this trend was maintained during autumn. By contrast, ocean temperatures off the west coast remained warmer than normal. Particularly warm temperatures were evident off the Gascoyne and southwest coasts of Western Australia, where anomalies were greater than +1.5 °C. For a discussion of Australian sea surface temperatures during the La Niña years of 2010 and 2011 see the report *State of the Climate 2012* at http://www.csiro.au/Outcomes/Climate/Understanding/State-of-the-Climate-2012/Oceans.aspx

All three standard monthly NINO indices increased during autumn. In the eastern Pacific the negative NINO3 index values warmed throughout autumn with the March value of –0.4 °C increasing to +0.1 °C by May. NINO3.4, indicative of conditions in the central Pacific, continued to warm slightly from –0.6 °C in March to –0.2 °C in May. Similarly, in the central to western Pacific, NINO4 increased from –0.5 °C in March to –0.3 °C in May. The largest warming took place in the far eastern Pacific, when NINO1+2 values rose from zero in March to +0.7 °C in April.

Fig. 5 Anomalies of SST for autumn 2011 (°C).

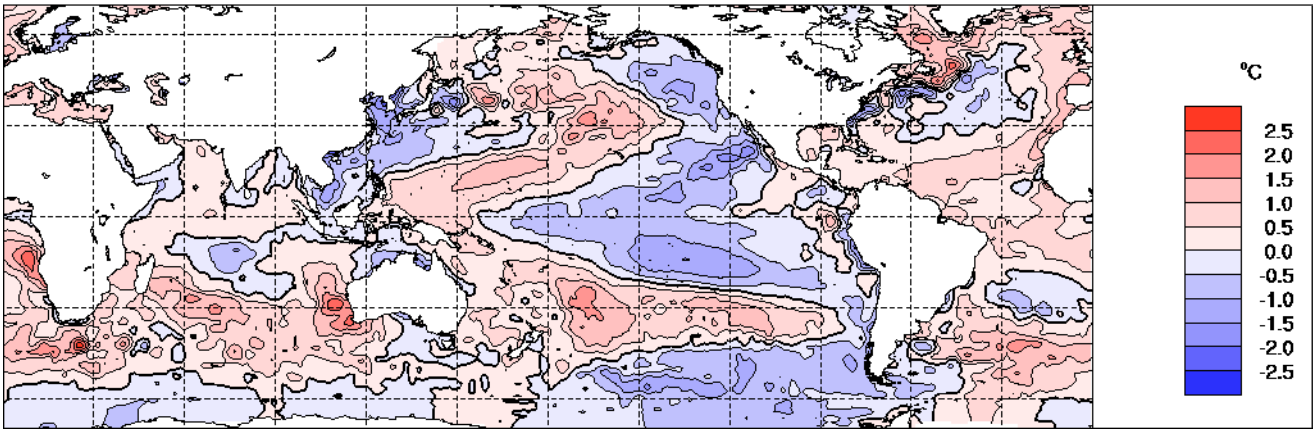

Subsurface ocean patterns

The Hovmöller diagram for the 20 °C isotherm depth anomaly along the equator from January 2004 to May 2011, obtained from NOAA's TAO/TRITON data[7], is shown in Fig. 6. The 20 °C isotherm depth is generally located close to the equatorial thermocline, which is the region of greatest temperature gradient with depth, and is the boundary between the warm near-surface and cold deep-ocean waters. Therefore, measurements of the 20 °C isotherm depth make a good proxy for the thermocline depth. Positive (negative) anomalies correspond to the 20 °C isotherm being deeper (shallower) than average. Changes in the thermocline depth may act as a precursor to subsequent temperature changes at the ocean surface. A shallow thermocline depth results in more cold water available for upwelling, and therefore a potential cooling of surface temperatures.

After the warming during the summer of 2009–10, the heat content of the Pacific basin decreased during 2010, as shown in Fig.5. The thermocline was anomalously shallow during the latter half of 2010 particularly over the eastern Pacific, indicating the onset of a major La Niña event. However, by late summer 2010–11, a warming of the subsurface was observed with the appearance of an anomalously deep 20 °C isotherm across the basin, initially west of the Date Line. This was associated with the propagation of a downwelling Kelvin wave which appeared during February 2011 and which propagated across the equatorial Pacific during autumn. Equatorially trapped downwelling Kelvin waves in the Pacific tend to increase the heat content of the ocean by depressing the thermocline[8]. The breakdown of the strong negative anomalies in the eastern Pacific in early 2011 is consistent with the life cycle decay of past La Niña events.

Figure 7 shows a cross-section of monthly equatorial subsurface anomalies from February 2011 to May 2011. Red shading indicates positive anomalies, and blue shading indicates negative anomalies. The subsurface cross-section shows a rapid collapse of the cool anomalies across the central and eastern Pacific which had been in place during the latter half of 2010. Warm anomalies of around +4 °C, which were present in the western and central Pacific, showed a weak decline during autumn. The pattern of the decaying cool subsurface temperature anomalies in autumn is consistent with the demise of past La Niña events.

Global atmospheric patterns

Surface analyses

The southern hemisphere autumn 2011 MSLP pattern, computed from the Bureau of Meteorology's Australian Community Climate and Earth-System Simulator[9] (ACCESS) model (the previous GASP model was phased out in August 2010), is shown in Fig. 8; the associated anomaly pattern is shown in Fig. 9. These anomalies are the difference from a 1979–2000 climatology obtained from the National Centers for Environmental Prediction (NCEP) II Reanalysis data (Kanamitsu et al. 2002). The MSLP analysis has been computed using data from the 0000 UTC daily analyses of the ACCESS model. The MSLP anomaly field is not shown over areas of elevated topography (grey shading).

The autumn 2011 MSLP pattern (Fig. 8) was zonal in the southern hemisphere mid- to high latitudes. The subtropical ridge was evident over southern Australia (1022.4 hPa), with centres of high pressure over the southern Indian Ocean (1021.6 hPa) and southwest Pacific (1021.3 hPa). The circumpolar low pressure belt can be seen in Fig. 8, with two low pressure minima of around 980 hPa in the southern Pacific. MSLP was higher than normal over the region south of Australia (an anomaly of +4.9 hPa), to the southeast of New Zealand (+6.4 hPa) and in the south Atlantic (+5.0 hPa), as shown in Fig. 9. The Australian continent was covered with weak positive anomalies and flanked to the east and west by weak negative anomalies.

[7]Hovmöller plot obtained from http://www.pmel.noaa.gov/tao/jsdisplay/
[8]http://iri.columbia.edu/climate/ENSO/theory/waves.html

[9]For more information on the Bureau of Meteorology's ACCESS model, see http://www.bom.gov.au/nwp/doc/access/NWPData.shtml

Fig. 6 Time-longitude section of the monthly anomalous depth of the 20 °C isotherm at the equator from January 2004 to May 2011. The contour interval is 10 m. (Plot sourced from TAO Project Office PMEL/NOAA)

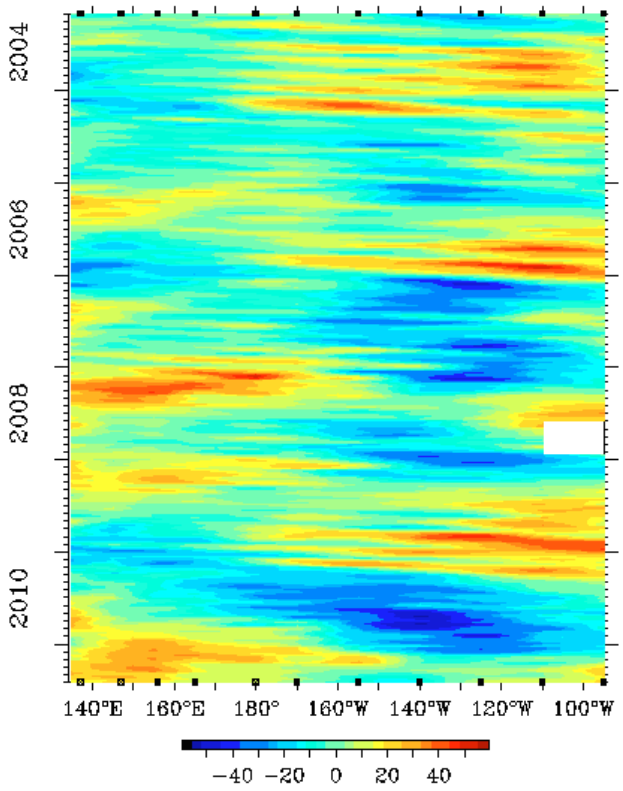

Fig. 7 Four-month February 2011 to May 2011 sequence of vertical ocean subsurface temperature anomalies at the equator for the Pacific Ocean (obtained from CAWCR).

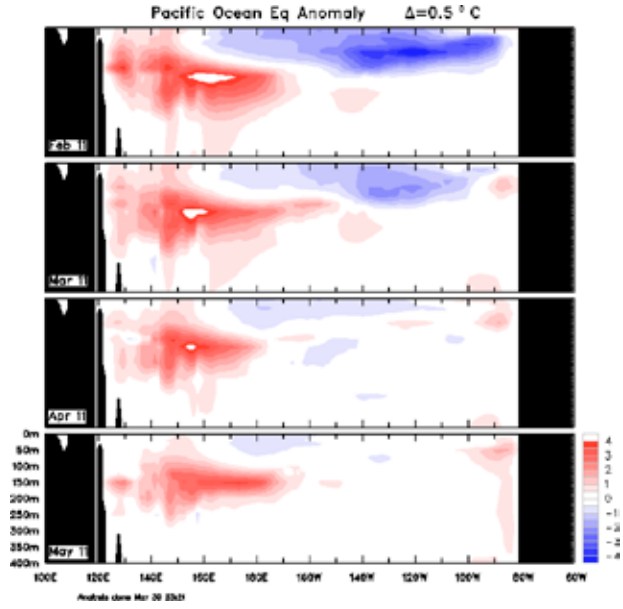

Mid-tropospheric analyses

The 500 hPa geopotential height, which is an indicator of the steering of surface synoptic systems across the southern hemisphere, for March to May 2011 is shown in Fig.10. The associated anomalies are shown in Fig. 11. Figure 10 displays the autumn 500 hPa heights showing the characteristic zonal pattern in the mid- to high latitudes, with weak hemispheric wave structure apart from the split flow in the east Australian region. The 500 hPa geopotential height anomalies were similar to the MSLP anomalies, with positive anomalies to the south of Australia and to the southeast of New Zealand. Negative anomalies were evident over eastern Australia as part of a blocking pattern, which was particularly evident during May with cyclonic activity in the Tasman Sea.

Southern Annular Mode

The Southern Annular Mode (SAM) describes the periodic, approximately ten-day, oscillation of atmospheric pressure between the polar and mid-latitude regions of the southern hemisphere. Positive phases of SAM are characterised by increased mass over the extra-tropics, decreased mass over Antarctica and a poleward contraction of the mid-latitude band of westerly winds. Conversely, negative phases of SAM relate to reduced mass over the extra-tropics, increased mass over Antarctica and an equatorward expansion of the mid-latitude band of westerly winds. A similar oscillation exists in the northern hemisphere, the Northern Annular Mode, or NAM (also known as the Arctic Oscillation). After being strongly positive during the previous winter and spring, the Climate Prediction Center standardised monthly SAM index (Climate Prediction Center 2010) dropped to neutral values during summer. The March and April values were –0.30 and –0.87 respectively, with the May value increasing to +1.27. The Southern Annular Mode has been shown to influence Australian temperature patterns (Hendon et al. 2007).

Blocking

The time–longitude section of the daily southern hemisphere blocking index (Wright 1993) is shown in Fig. 12, with the start of the season beginning at the top of the plot. This index is a measure of the strength of the zonal 500 hPa flow in the mid-latitudes (40ºS to 50ºS) relative to that at lower (25ºS to 30ºS) and higher (55ºS to 60ºS) latitudes. Positive values of the blocking index are generally associated with a split in the mid-latitude westerly flow centred near 45ºS and mid-latitude blocking activity. Blocking activity most commonly occurs in the Australian and western Pacific longitudes. Figure 13 shows the seasonal index for each longitude.

The seasonal index shows that blocking was above average in the Indian Ocean and in Australian longitudes and below normal across the South Pacific. There were several blocking episodes during autumn in the Australian region. Most of these were the result of cut-off low activity in the Tasman Sea with large anticyclones south of their normal track to the south of Australia and in the southern Tasman Sea (Fig. 12).

Fig. 8 Autumn 2011 MSLP (hPa).

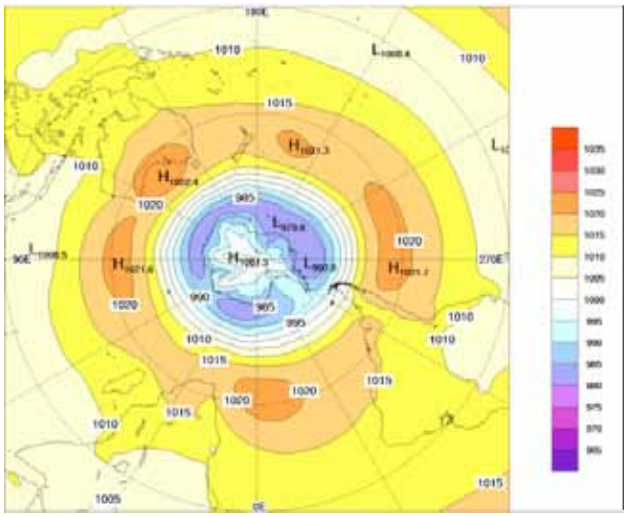

Fig. 9 Autumn 2011 MSLP anomalies (hPa).

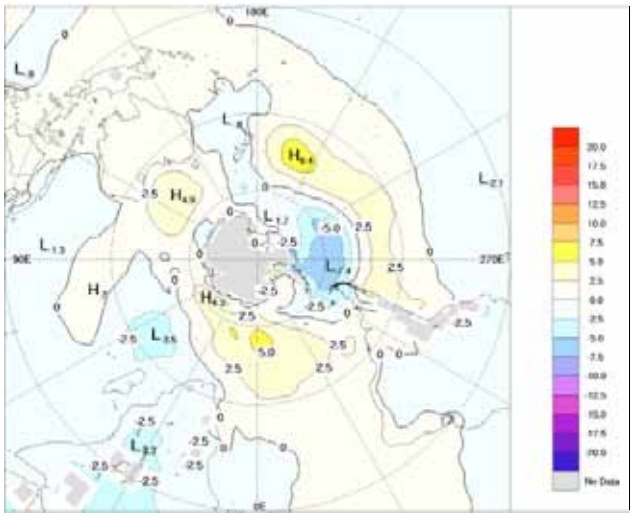

Fig. 10 Autumn 2011 500 hPa mean geopotential height (gpm). The contour interval is 100 gpm.

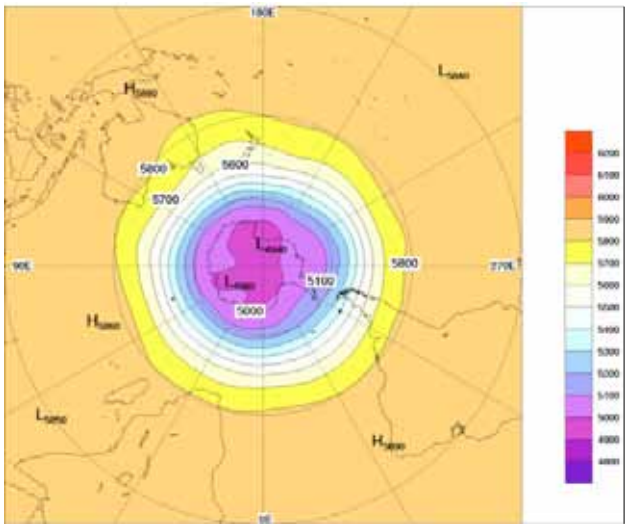

Fig. 11 Autumn 2011 500 hPa mean geopotential height anomalies (gpm). The contour interval is 30 gpm.

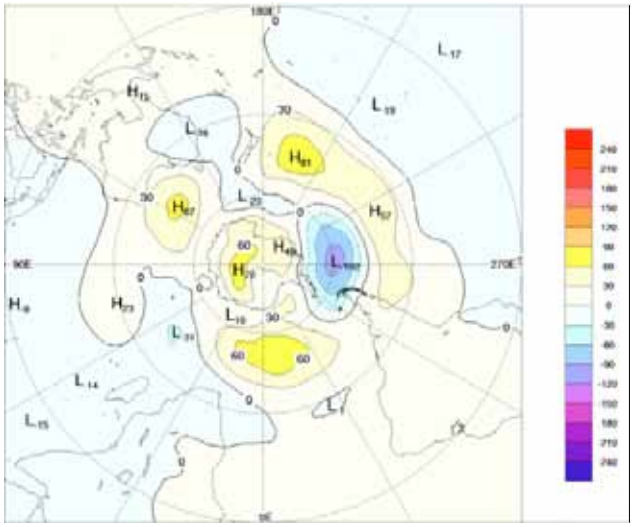

Winds

Autumn 2011 low-level (850 hPa) and upper-level (200 hPa) wind anomalies (as per the surface analyses, computed from ACCESS and anomalies with respect to the 22-year NCEP II climatology) are shown in Figs 14 and 15, respectively. Isotach contours are at 5 m s^{-1} intervals.

Easterly low-level wind anomalies continued over the central and western tropical Pacific Ocean, while there were westerly wind anomalies over Indonesia and northern Australia and in the far eastern tropical Pacific. Enhanced upper-level westerly wind anomalies (~20 m s^{-1}) over the west and central equatorial Pacific combined with weak easterly anomalies over the Maritime Continent were indicative of a stronger than normal Walker Circulation, which is characteristic of a La Niña and was particularly evident during the earlier half of autumn. The low-level wind anomalies show an anticyclonic anomaly to the south of Australia and a cyclonic anomaly off the Australian east coast, indicative of the enhanced blocking in the Australian region.

Australian region

Rainfall

Australian rainfall totals for autumn 2011 are shown in Fig. 16, while the rainfall deciles for the same period are shown in Fig. 17. The rainfall deciles are calculated using all autumns from 1900 to 2011.

There were notable contrasts in the autumn rainfall patterns across Australia. (Fig. 17, Table 1). Nationally averaged rainfall was 205.3 mm (70 per cent above normal), the fourth-highest on record for autumn (the highest was 227.4 mm in 1989), and the highest since 2000. The Northern

Fig. 12 Autumn 2011 daily southern hemisphere blocking index (m s^{-1}) time-longitude section. The horizontal axis shows degrees east of the Greenwich meridian. Day one is 1 March.

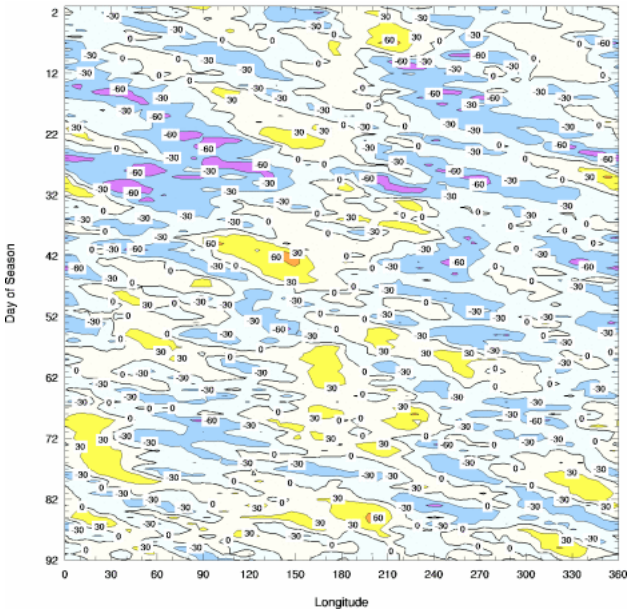

Territory recorded its wettest autumn with a territory-wide average of 341.0 mm (145 per cent above normal), exceeding the previous 1983 record of 304.8 mm. Queensland recorded 284.1 mm (74 per cent above normal), the highest since 1990.

Areas of very-much-above-average rainfall were widespread across Australia. Almost the entire Northern Territory, Queensland and South Australia received well-above-normal falls, with many areas recording highest-on-record autumn rainfall. By contrast, the western halves of Western Australia and Tasmania reported modest rainfall deficiencies. Some areas over the southwest corner of Western Australia ranked lowest on record in March.

The 2010–11 La Niña, one of the strongest La Niña events on record, started to decline during autumn. Nevertheless, its influence continued to be felt during March and the first half of April with an active monsoon trough over northern Australia which penetrated southwards.

Following the very active tropical cyclone season of the summer, there was only one named tropical cyclone in the Australian region during autumn. Tropical cyclone *Errol* formed in the Timor Sea during mid-April and briefly reached category 2 strength before moving away from the Western Australian coast. Prior to this in early April, a low pressure system developed over the Joseph Bonaparte Gulf and produced heavy rainfall and storms across the western Top End. As the low moved southwest parallel to the north Kimberley coast, the axis of the monsoon trough also moved south, bringing further heavy rain to the area. The heavy rainfall during the first week of the month set new daily and monthly rainfall records for many stations across the Top End.

Fig. 13 Mean southern hemisphere blocking index (m s^{-1}) for autumn 2011 (solid line). The dashed line shows the corresponding long-term average. The horizontal axis shows degrees east of the Greenwich meridian.

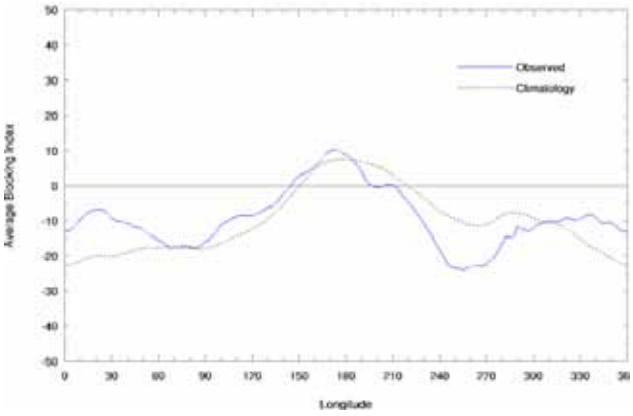

Drought

Above- to very-much-above-average rainfall across most of Australia during summer and early autumn eased short term rainfall deficiencies. Rainfall in previous seasons in southwest Western Australia was very much below average with the area experiencing persistent rainfall deficiencies. Summer and autumn rainfall was insufficient to make significant inroads into those deficiencies. For example, during the year to the end of May 2011 the southwestern divisions of Western Australia experienced very-much-below-average rainfall with many areas ranked as lowest on record. Similarly, for the 18-month period from December 2009 to May 2011, the southwestern divisions of Western Australia experienced serious rainfall deficiencies with many locations reporting lowest on record, as seen in Fig.18. The deficiencies discussed above occurred against a backdrop of decade-long rainfall deficits in southwest Western Australian and high temperatures that have stressed water supplies.

Temperature

Figure 19 shows maximum and minimum temperature anomalies for autumn 2011. Seasonal anomalies are calculated with respect to the 1961–1990 period, and use all stations for which an elevation is available. Station normals have been estimated using gridded climatologies for those stations with insufficient data within the 1961–1990 period to calculate a station normal directly. Figure 19 shows maximum and minimum temperature deciles, calculated using monthly temperature analyses from 1911 to 2010.

Maximum temperatures averaged over Australia were 1.40 °C below normal for autumn, making it the second-coolest autumn in the post-1950 period (the coolest was in 2000, with an anomaly of –1.46 °C). Most of Australia recorded below-average maximum temperatures, apart from the west coast of Western Australia and the adjacent hinterland where maxima were more than 1 °C above normal. The Northern Territory recorded its lowest autumn maximum temperature

Fig. 14 Autumn 2011 850 hPa vector wind anomalies (m s^{-1}).

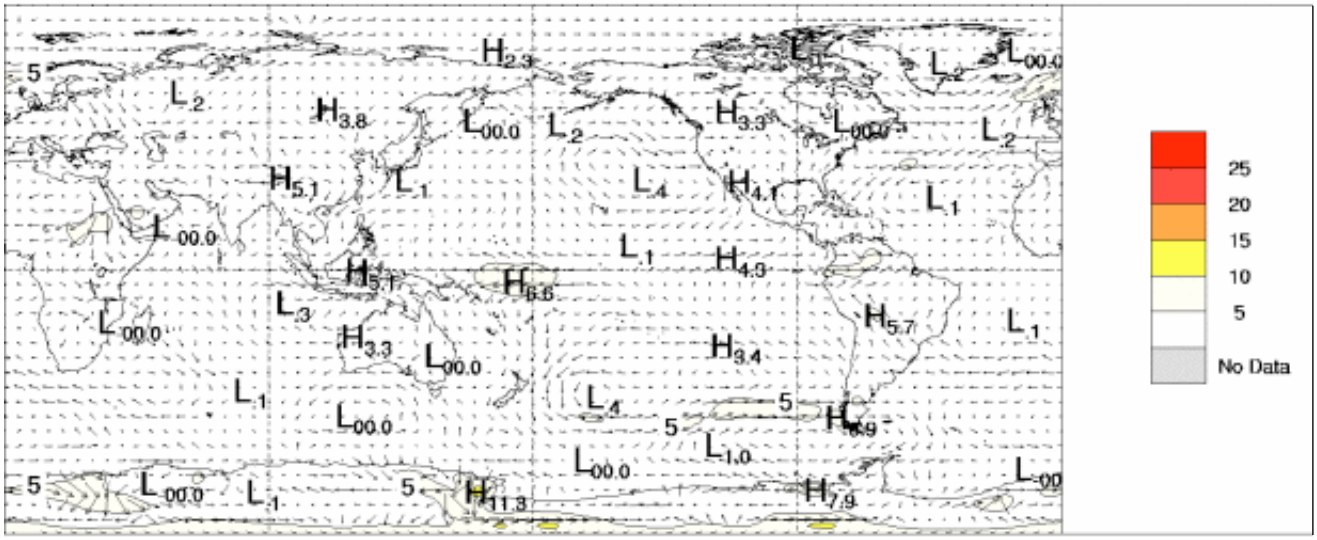

Fig. 15 Autumn 2011 200 hPa vector wind anomalies (m s^{-1}).

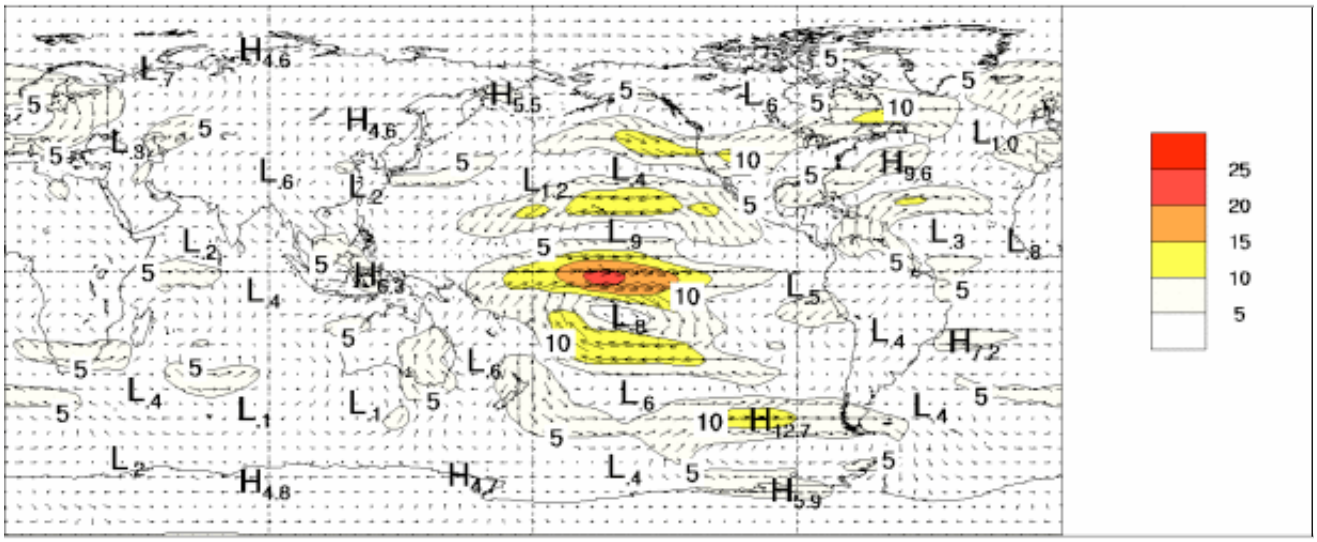

Fig. 16 Autumn 2011 rainfall totals (mm) for Australia.

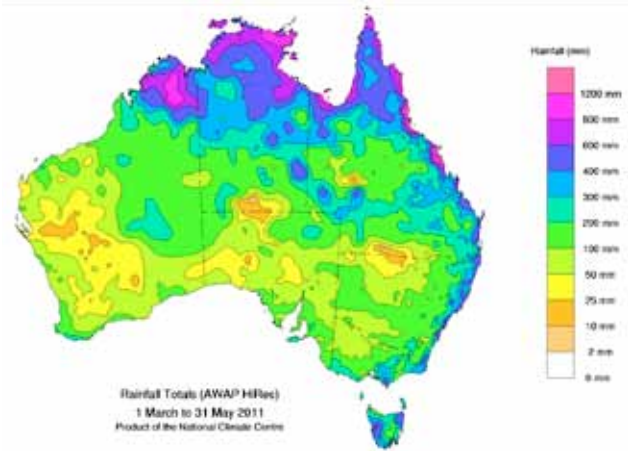

Fig. 17 Autumn 2011 rainfall deciles for Australia. Deciles ranges based on grid-point values over the autumns 1900–2011.

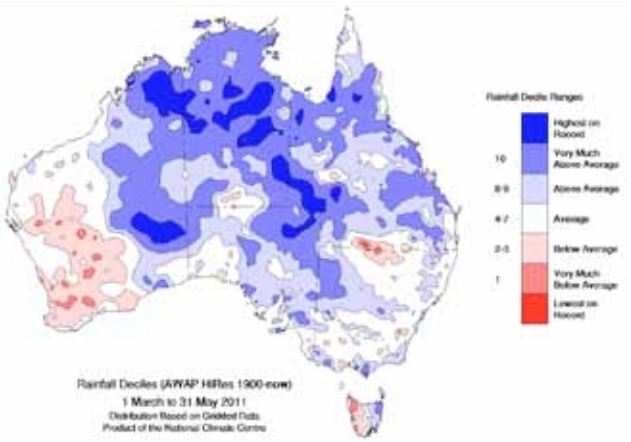

Fig. 18 December 2009 to May 2011 rainfall deciles for Western Australia. Deciles ranges based on grid-point values over the December to May periods 1900–2011.

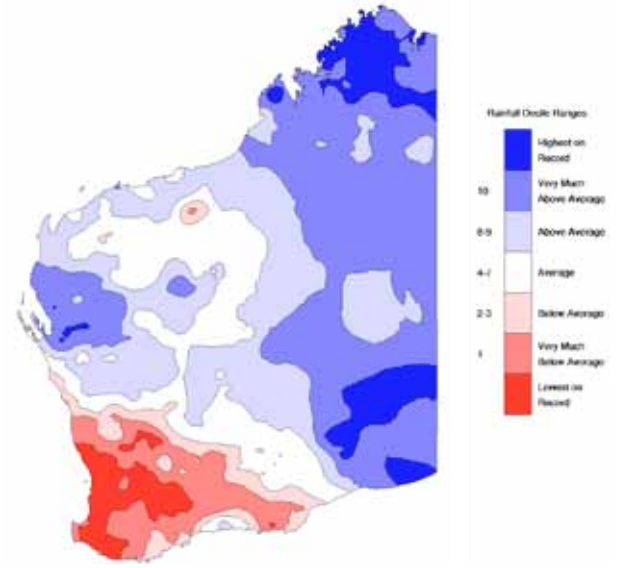

Fig. 19 Autumn 2011 temperature anomalies (°C): (a) Maximum temperature anomalies; and (b) Minimum temperature anomalies.

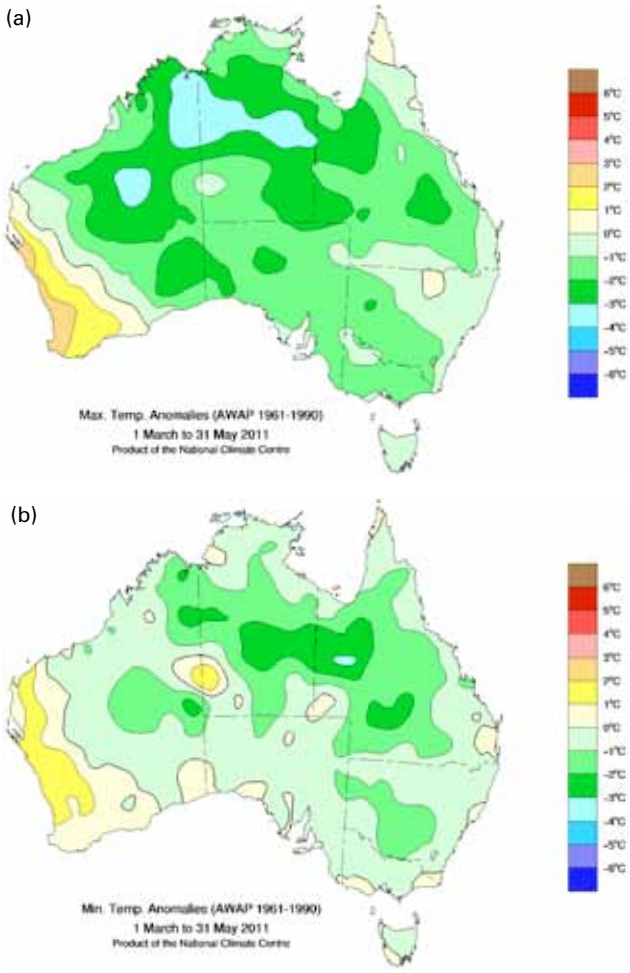

anomaly (–2.55 °C), eclipsing the previous record of –2.11 °C set in 2000. The Northern Territory experienced its coolest March on record (–3.4 °C) with several stations recording their lowest mean maximum. Many new low maximum temperature records were set in March in South Australia (statewide anomaly of –2.9 °C), contributing to a second-lowest South Australian autumn maximum temperature anomaly of –1.62 °C, compared to the record of –2.08 °C set in autumn 1955. Victoria recorded its fourth-lowest autumn maximum temperature anomaly, –1.09 °C, the lowest since the record of –1.72 °C was set in 1995.

Most of Australia experienced negative minimum temperature anomalies during autumn; the season was the fifth-lowest on record for the nation as a whole (–0.9 °C). The largest negative anomalies were over the Northern Territory (–1.94 °C, the lowest on record for the Territory) and Queensland (–1.31 °C, the fourth-lowest on record).

Australia-wide mean temperatures for autumn 2011 were the coolest on record (–1.15 °C), eclipsing the previous record –0.95 °C, set in 1960. Major contributions were from the Northern Territory (–2.24 °C) and Queensland (–1.27 °C), both of which set new low mean temperature records.

Fig. 20 Autumn 2011 temperature deciles for Australia. Decile ranges based on grid-point values over the autumn periods for 1900–2011: (a) Maximum temperature deciles; and (b) Minimum temperature deciles.

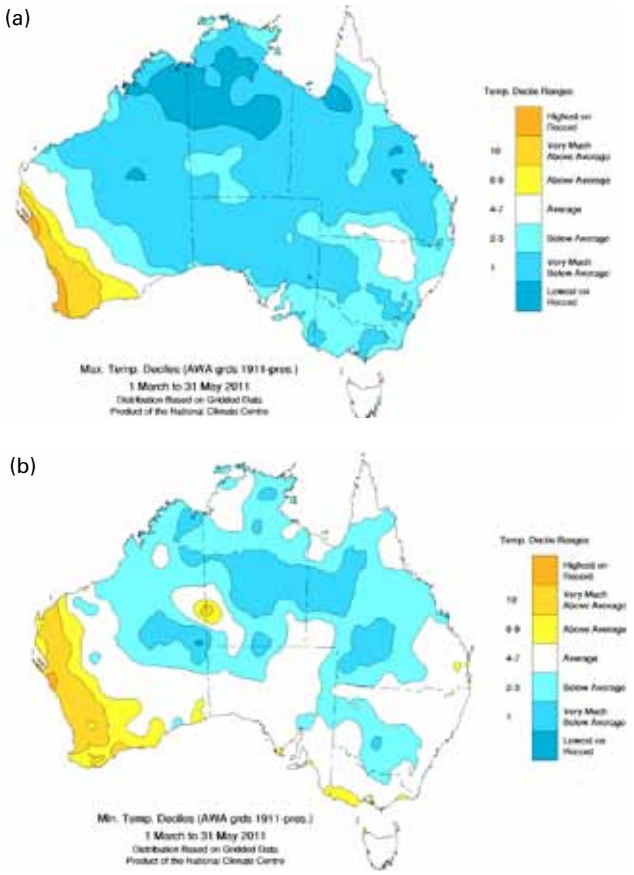

Table 1. Summary of the seasonal rainfall ranks and extremes on a national and State basis for autumn 2011. The ranking in the last column goes from 1 (lowest) to 112 (highest) and is calculated over the years 1900–2011.

Region	*Highest seasonal total (mm)*	*Lowest seasonal total (mm)*	*Highest daily total (mm)*	*Area-average rainfall (mm)*	*Rank of area-averaged rainfall*
Australia	2540 at Bellenden Ker Top Station (Qld)	9 at Nilpinna (SA)	477 at Mornington Island (Qld), 1 March	205	109
Queensland	2540 at Bellenden Ker Top Station	21 at Bulloo Downs	477 at Mornington Island, 1 March	284	16
New South Wales	810 at Careys Peak (Barrington Tops)	17 at Enngonia (Shearer Street)	398 at Cathcart (Mount Darragh), 22 March	137	78
Victoria	552 at Wyelangta	48 at Bridgewater (Post Office)	140 at Thorpdale Peak, 23 March	153	68
Tasmania	800 at Mount Read	70 at Ouse Fire Station	327 at Gray (Dalmayne Rd), 24 March	310	10
South Australia	329 at Crafers (Mt Lofty)	9 at Nilpinna	170 at Marree (Dulkaninna), 8 March	92	102
Western Australia	961 at Durack Range	12 at Depot Springs	351 at Durack Range, 14 March	148	102
Northern Territory	1430 at Lake Evella	13 at Kulgera	196 at Lake Evella, 22 March	341	112

Table 2. Percentage areas in different categories for autumn 2011 rainfall. 'Severe deficiency' denotes rainfall at or below the 5th percentile. Areas in 'decile 1' include those in 'severe deficiency', which in turn include those which are 'lowest on record'. Areas in 'decile 10' include those which are 'highest on record'. Percentage areas of highest and lowest on record are given to two decimal places because of the small quantities involved: other percentage areas to one decimal place.

Region	*Lowest on record*	*Severe deficiency*	*Decile 1*	*Decile 10*	*Highest on record*
Australia	0.00	0.0	0.3	47.9	8.61
Queensland	0.00	0.0	0.0	61.5	5.46
New South Wales	0.00	0.0	0.2	16.0	0.00
Victoria	0.00	0.0	0.0	6.1	0.00
Tasmania	0.00	0.0	4.5	28.1	0.92
South Australia	0.00	0.0	0.0	40.5	2.40
Western Australia	0.00	0.0	0.7	36.7	10.77
Northern Territory	0.00	0.0	0.0	84.8	20.55

Table 3. Summary of the seasonal maximum temperature ranks and extremes on a national and State basis for autumn 2011. The ranking in the last column begins from 1 (lowest) to 62 (highest) and is calculated over the years 1950–2011.

Region	*Highest seasonal mean maximum (°C)*	*Lowest seasonal mean maximum (°C)*	*Highest daily temperature (°C)*	*Lowest daily maximum temperature (°C)*	*Area-averaged temperature anomaly (°C)*	*Rank of area-averaged temperature anomaly*
Australia	34.1 at Emu Creek (WA)	7.5 at Mount Hotham (Vic)	41.9 at Birdsville (Qld), 1 March	–4.6 at Thredbo Top Station (NSW), 11 May	–1.40	2
Queensland	32.0 at Scherger RAAF	19.8 at Applethorpe	41.9 at Birdsville, 1 March	9.4 at Applethorpe, 25 May	–1.23	5
New South Wales	27.8 at Mungindi	8.2 at Thredbo Top Station	41.4 at Walgett, 1 March	–4.6 at Thredbo Top Station, 11 May	–0.62	10
Victoria	22.5 at Swan Hill	7.5 at Mount Hotham	34.5 at Hopetoun, 7 March	–4.1 at Mount Hotham, 11 May	–1.09	4
Tasmania	18.5 at Eddystone Point	8.2 at Mount Wellington	30.8 at Ouse, 12 March	–0.5 at Mount Wellington, 4 March	+0.04	34
South Australia	27.7 at Moomba	15.8 at Mount Lofty	39.0 at Marree Comparison, 16 March	8.2 at Mount Lofty, 25 May	–1.62	2
Western Australia	34.1 at Emu Creek	22.1 at Albany	41.1 at Roebourne, 19 March	14.0 at Shannon, 20 May	–1.13	6
Northern Territory	32.6 at Jabiru	24.9 at Arltunga	37.8 at Walungurru, 7 March	14.8 at Arltunga, 26 May	–2.55	1

Table 4. Summary of the seasonal minimum temperature ranks and extremes on a national and State basis for autumn 2011. The ranking in the last column begins from 1 (lowest) to 62 (highest) and is calculated over the years 1950–2011.

Region	*Highest seasonal mean minimum (°C)*	*Lowest seasonal mean minimum (°C)*	*Highest daily minimum temperature (°C)*	*Lowest daily temperature (°C)*	*Area-averaged temperature anomaly (°C)*	*Rank of area-averaged temperature anomaly*
Australia	25.4 at Varanus Island (WA)	0.7 at Perisher Valley (NSW)	31.1 at Murchison (WA), 1 March	–9.0 at Woolbrook (NSW), 15 May	–0.90	5
Queensland	25.2 at Coconut Island	9.5 at Applethorpe	28.2 at Birdsville, 2 March	–2.8 at Applethorpe, 15 May	–1.31	4
New South Wales	17.2 at Cape Byron	0.7 at Perisher Valley	28.3 at Tiboobura Post Office, 1 March	–9.0 at Woolbrook, 15 May	–0.81	15
Victoria	13.3 at Gabo Island	1.8 at Mount Hotham	22.0 at Port Fairy, 8 March	–6.7 at Falls Creek, 12 May	–0.49	27 (tied)
Tasmania	12.7 at Hogan Island	1.7 at Liawenee	18.8 at Hogan Island, 13 March	–7.4 at Liawenee, 10 May	–0.05	35 (tied)
South Australia	15.0 at Neptune Island	7.6 at Yongala	28.0 at Oodnadatta, 1 March	–4.2 at Yunta, 16 May	–0.28	25 (tied)
Western Australia	25.4 at Varanus Island	9.5 at Jarrahwood	31.1 at Murchison, 1 March	–2.4 at Eyre, 28 May	–0.39	16
Northern Territory	24.0 at Black Point	11.0 at Alice Springs	28.2 at Black Point, 2 March	–4.2 at Arltunga, 31 May	–1.94	2

References

Campbell, B. 2011. Seasonal climate summary southern hemisphere (autumn 2010): rapid decay of El Niño, wetter than average in central, northern and eastern Australia and warmer than usual in the west and south. *Aust. Met. and Oceanogr. J., 61,* 65–76.

Climate Diagnostics Center. 2011. *Historical ranks of the MEI*, http://www.cdc.noaa.gov/people/klaus.wolter/MEI/rank.html.

Climate Prediction Center. 2011. *Monthly mean AAO index since January 1979*.

Donald, A., Meinke, H., Power, B., Wheeler, M. and Ribbe, J. 2004. Forecasting with the Madden–Julian Oscillation and the applications for risk management. In: *4th International Crop Science Congress,* 26 September – 01 October 2004, Brisbane, Australia

Ganter, C. 2010. Seasonal climate summary southern hemisphere (winter 2010): A fast developing La Niña. *Aust. Met. and Oceanogr. J., 61,* 125–35.

Hendon, H., Thompson D.W.J. and Wheeler M.C, 2007: Australian Rainfall and Surface Temperature Variations Associated with the Southern Hemisphere Annular Mode. *J. Clim., 20,* 2452–67. doi: http://dx.doi.org/10.1175/JCLI4134.1

Imielska, A. 2011. Seasonal climate summary southern hemisphere (summer 2010–2011): second-wettest Australian summer on record and one of the strongest La Niña events on record. *Aust. Met. and Oceanogr. J., 61,* 241–51.

Kanamitsu, M., Ebisuzaki, W., Woollen, J., Yang, S.-K., Hnilo, J.J., Fiorino, M. and Potter, G.L. 2002. NCEP-DOE AMIP-II Reanalysis (R-2). *Bull. Am. Meteorol. Soc., 83,* 1631–43.

Kuleshov, Y., Qi, L., Fawcett, R. and Jones, D. 2009. "Improving preparedness to natural hazards: Tropical cyclone prediction for the Southern Hemisphere," in: Gan, J. (Ed.), *Advances in Geosciences*, Vol. 12 Ocean Science, World Scientific Publishing, Singapore, 127–43.

Lovitt, C. 2011 Seasonal climate summary southern hemisphere (spring 2011): La Niña strengthens. *Aust. Met. and Oceanogr. J., 61,* 185–95.

Reynolds, R.W., Rayner, N.A., Smith, T.M., Stokes, D.C. and Wang, W. 2002. An improved in situ and satellite SST analysis for climate. *J. Clim., 15,* 1609–25.

Troup, A.J. 1965. The Southern Oscillation. *Q.J.R Meteorol. Soc., 91,* 490–506.

Wolter, K. and Timlin, M.S. 1993. Monitoring ENSO in COADS with a seasonally adjusted principal component index. *Proc. of the 17th Climate Diagnostics Workshop*, Norman OK, NOAA/NMC/CAC, NSSL, Oklahoma Clim. Survey, CIMMS and the School of Meteorology, Univ. of Oklahoma, 52–7.

Wolter, K. and Timlin, M.S. 1998. Measuring the strength of ENSO – how does 1997/98 rank? *Weather, 53,* 315–24.

Wheeler, M.C., Hendon, H.H., Cleland, S., Meinke, H. and Donald, A. 2009: Impacts of the Madden–Julian Oscillation on Australian Rainfall and Circulation. *J. Clim., 22,* 1482–98. doi: http://dx.doi.org/10.1175/2008JCLI2595.1

Wright, W.J. 1993. Seasonal climate summary southern hemisphere (autumn 1992): signs of a weakening ENSO event. *Aust. Meteorol. Mag., 42,* 191–98.

Zhang, C. 2005, Madden–Julian Oscillation, *Rev. Geophys., 43,* RG2003, doi:10.1029/2004RG000158.